# Identification of novel small-molecule inhibitors of α-methylacyl-CoA racemase (AMACR; P504S) and structure-activity relationships

Yoana D. Petrova[a], Katty Wadda[a,b], Amit Nathubhai[a,c], Maksims Yevglevskis[a], Paul J. Mitchell[a], Tony D. James[b], Michael D. Threadgill[a], Timothy J. Woodman[a], Matthew D. Lloyd[a],

[a] Drug & Target Discovery, Department of Pharmacy & Pharmacology, University of Bath, Claverton Down, Bath BA2 7AY, UK
[b] Department of Chemistry, University of Bath, Claverton Down, Bath BA2 7AY, UK
cSchool of Pharmacy and Pharmaceutical Sciences, Sciences Complex, City Campus, Dale Building, Room 121, Sunderland SR1 3SD, UK[1]

## ARTICLE INFO

## ABSTRACT

α-Methylacyl-CoA racemase (AMACR; P504S; EC 5.1.99.4) catalyses epimerization of 2-methylacyl-CoAs and is important for the degradation of branched-chain fatty acids and the pharmacological activation of ibuprofen and related drugs. It is also a novel drug target for prostate and other cancers. However, development of AMACR as a drug target has been hampered by the difficulties in assaying enzyme activity. Consequently, reported inhibitors have been rationally designed acyl-CoA esters, which are delivered as their carboxylate prodrugs. The novel colorimetric assay for AMACR based on the elimination of 2,4-dinitrophenolate was developed for high-throughput screening and 20,387 'drug-like compounds' were screened, with a throughput of 768 compounds assayed per day. Pyrazoloquinolines and pyrazolopyrimidines were identified as novel scaffolds and investigated as AMACR inhibitors. The most potent inhibitors have $IC_{50}$ values of ~2 μM. The pyrazoloquinoline inhibitor **10a** displayed uncompetitive inhibition, whilst **10j** displayed mixed competitive inhibition. The pyrazolopyr-imidine inhibitor **11k** displayed uncompetitive inhibition. This is the first report of the identification of specific drug-like small-molecule AMACR inhibitors by high-throughput screening. Pyrazoloquinolines and pyr-azolopyrimidines may also be useful as inhibitors of other CoA-utilizing enzymes.

## 1. Introduction

Branched-chain fatty acids are common in the diet and derivatives thereof are used as medicines. 2-Methyl-fatty acids are derived catabolically from dietary 3-methyl-fatty acid precursors (*e.g.* phytanic acid) or are made endogenously (*e.g.* the bile acids derived from cholesterol) [1–4]. The β-oxidation pathway, which degrades 2-methyl fatty acids, can only process *S*-2-methylacyl-CoAs [5–7] but a mixture of *R*- and *S*-2-methylacyl-CoAs are produced from phytanic acid [3], whilst bile acids are predominantly produced as *R*-2-methylacyl-CoAs [1,8]. The enzyme α-methylacyl-CoA racemase (AMACR; P504S; EC 5.1.99.4) catalyses conversion of *R*-2-methylacyl-CoAs to a near 1:1 epimeric mixture of 2-methylacyl-CoAs [9,10] by a deprotonation/re-protonation reaction [9–12], probably *via* an enolate intermediate [13,14]. The resulting *S*-2-methylacyl-CoAs undergo β-oxidation, whilst the remaining *R*-2-methylacyl-CoAs are further converted to their 2*S*

epimers by AMACR, allowing their complete degradation [1–4]. AMACR is also involved in the pharmacological activation of ibuprofen and similar drugs [1,2,10].

AMACR protein levels are increased in prostate cancer [15,16], breast cancer [17], myxofibrosarcomas [18], some colon cancers [19] and various other cancers [1,20]. Increased catalytic activity has also been reported in prostate cancers [16,21]. Reducing protein levels of active spliced variants in prostate cancer cell lines results in reduced proliferation [21,22], which is synergistic with deprivation of andro-gens [21]. Some advanced prostate cancer cell lines revert from an-drogen-independent to androgen-dependent growth upon knock-down of AMACR [23]. Intriguingly, long-term use of low dose ibuprofen ap-pears to reduce the risk of prostate [24] and colon cancer [25] in pa-tients with particular AMACR single-nucleotide polymorphisms (SNPs). Consequently, there has been considerable interest in AMACR as both a drug target and cancer marker.
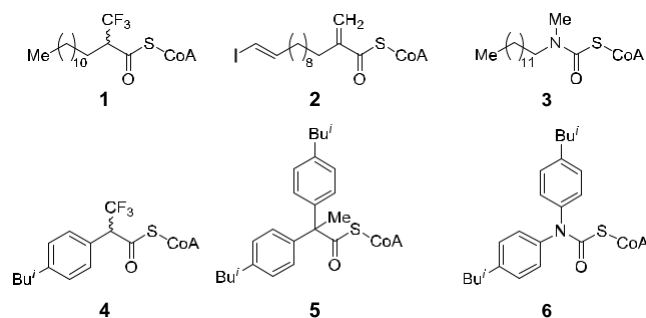
**Fig. 1.** Examples of previously reported rationally designed AMACR inhibitors **1**–**4** [29–32] and inhibitors **5** and **6** of MCR [33,34], the *M. tuberculosis* homologue of AMACR.

Development of AMACR as a drug target has been difficult because of the lack of an X-ray crystal structure of the human enzyme (although structures of the *M. tuberculosis* homologues, MCR [11–13] and FAR [26], have been reported), and because of the difficulties of assaying the enzyme [27,28]. Therefore, the majority of studies have focused on rational drug design strategies to produce inhibitors of AMACR (ex-amples shown in Fig. 1, **1**–**4**) [29–32] or its bacterial homologue, MCR (examples shown in Fig. 1, **5** and **6**) [33,34]. These studies have pro-duced highly potent acyl-CoA inhibitors [29–32] but these do not comply with Lipinski's guidelines [35,36] and must be delivered to cells as their carboxylic acid precursors. Only one study has investigated the use of a screening approach to identify inhibitors [22]. The authors of this study successfully screened a library of ~5000 compounds, and identified a number of non-specific protein modification agents as in-hibitors of AMACR [2,22]. However, the assay was discontinuous, used a labelled substrate with measured rates subject to a kinetic isotope effect, and was labour-intensive. Consequently, this assay is not well-suited for screening large libraries of drug-like compounds.

We recently reported the development of a novel continuous col-orimetric assay for the measurement of AMACR activity [28]. This assay is based on the use of a colourless substrate **7**, which eliminates 2,4-dinitrophenolate **8** (which is intensely yellow) and forms un-saturated product **9** (Scheme 1). This assay was previously used to examine structure-activity relationships of known inhibitors and other acyl-CoAs known to bind to AMACR [28,37]. Herein, we report a study in which this assay was used to screen libraries containing 20,387 drug-like' molecules, identify novel AMACR inhibitors and examine struc-ture-activity relationships.

## 2. Results and discussion

### 2.1. Screening strategy for inhibitors

The colorimetric assay was selected for development for high-throughput screening applications, owing to its irreversible conversion of substrate to products and the ability to follow continuously the for-mation of 2,4-dinitrophenolate **8** at 354 nm. A substrate concentration of 40 μM was chosen, as this is close to the reported $K_m$ value for substrate **7** [28,37]. These 'balanced conditions' result in equal pro-portions of free enzyme and enzyme-substrate complex and facilitates identification of inhibitors with diverse kinetic mechanisms [38]. There
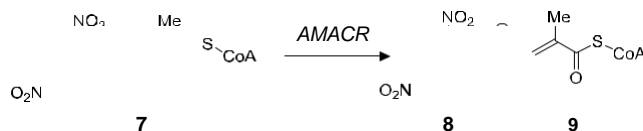


**Scheme 1.** Elimination of colorimetric substrate **7** by AMACR to give yellow 2,4-dinitrophenolate **8** and unsaturated product **9**.

was considerable variation in the background absorbance at 354 nm between different microtitre plate wells and hence formation of product was followed using a time course, typically of 8 min. This also improved the ease of analysing compounds which had significant absorbance at 354 nm. Under the standard assay conditions (see Experimental for details), a robustness (Z′ factor [39]) of 0.71 ± 0.13 was calculated. This compares with previously reported value of 0.906 [28]. The sta-tistical parameters for the assay (Supporting Information, Table S1) show that it is suitable for the identification of AMACR inhibitors.

Two libraries of compounds were obtained from LifeArc (formerly MRC technology). A library containing 10,419 molecules designed to interact with the hinge-region ATP-binding pocket of kinases was chosen. As ATP and CoA share a common nucleotide structure, it was thought that 'kinase-like' inhibitors would compete with the adenosine moiety of the acyl-CoA substrate. The second library of compounds was the index set, containing a clustered collection of 9968 drug-like mo-lecules [40]. Compounds were supplied as 1.0 mM stock solutions in DMSO and were used at a final concentration of 30 μM in the assay [also giving a final concentration 3.0% (v/v) DMSO in each well]. Potential inhibitors were incubated with enzyme for 10 min before addition of substrate, in order to allow time for the enzyme-inhibitor complex to form. Potential hits were re-assayed to confirm the dimin-uation in enzyme activity and were compared with positive (en-zyme + DMSO) and negative (buffer + DMSO) controls. Use of two 96-well plates in tandem with an 8-min time course allowed screening of 768 library wells (2 × 384 plates of inhibitor) per day and this could be increased to 1152 library wells (three plates) per day. Using this pro-tocol, 89 hits (~0.4%) were initially identified for further investigation. The compounds identified were triaged based on Lipinski guidelines (LogP = < 5, $M_W$ = < 500 [35,36] and 'frequent hitter' status [41,42]. From this analysis, pyrazoloquinolines **10a-10q** (Table 1) and

**Table 1**

IC$_{50}$ values for the series of pyrazoloquinoline inhibitors **10** as measured by the colorimetric assay [28] and calculated lipophilicity. IC$_{50}$ values are expressed as geometric means for three independent repeats with lower and upper geo-metric standard error of the Mean values in parentheses (see Experimental for details).
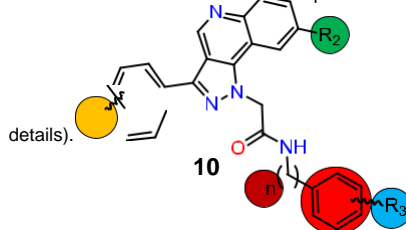


| | R$^1$ | R$^2$ | R$^3$ | n | Ring | IC$_{50}$ (μM) | Calc. LogP[b] |
|---|---|---|---|---|---|---|---|
| **10a** | H | F | H | 0 | Ph | 2.24 (1.93, 2.59) | 3.77 |
| **10b** | 4-F | F | H | 0 | Ph | 7.41 (6.25, 8.77) | 3.93 |
| **10c** | 4-OMe | F | H | 0 | Ph | 13.7 (12.1, 15.5) | 3.82 |
| **10d** | 3-F | H | H | 0 | Ph | 8.05 (7.67, 8.44) | 4.74 |
| **10e** | 4-F | Me | 4-OMe | 0 | Ph | ≫50 | 5.25 |
| **10f** | 4-F | Me | 3-F | 0 | Ph | 41.5 (16.7, 102) | 5.33 |
| **10g** | 4-F | Me | 3-Me | 0 | Ph | 4.00 (3.35, 4.78) | 5.61 |
| **10h** | 4-F | Me | 3-OMe | 0 | Ph | 5.77 (5.08, 6.55) | 5.22 |
| **10i** | 4-F | OMe | H | 0 | Ph | 1.80 (1.52, 2.14) | 4.80 |
| **10j** | 4-F | F | 4-F | 0 | Ph | 1.52 (1.40, 1.66) | 4.09 |
| **10k** | 4-F | F | 3-F | 0 | Ph | 4.47 (3.67, 5.45) | 4.07 |
| **10l** | 4-F | H | 3-F | 0 | Ph | 6.31 (5.81, 6.84) | 4.88 |
| **10m** | 4-F | F | 2-F | 0 | Ph | ≫50 | 4.05 |
| **10n** | 4-F | F | 3,4 di-F | 0 | Ph | 7.55 (6.74, 8.46) | 5.00 |
| **10o** | 4-F | F | 3-OMe | 0 | Ph | No activity[a] | 3.96 |
| **10p** | 4-F | F | H | 0 | cHex | 17.5 (13.1, 23.5) | 4.14 |
| **10q** | 4-F | F | H | 1 | Ph | ≫50 | 3.63 |

[a] No activity means < 5% inhibition observed at highest concentration of compound [50 μM in 3.0% (v/v) DMSO].

[b] LogP values calculated using http://www.molinspiration.com/cgi-bin/properties.

**Table 2**

IC$_{50}$ values for the series of pyrazolopyrimidine inhibitors **11a**–**11k** as mea-sured by the colorimetric assay [28] and calculated lipophilicity. IC$_{50}$ values are expressed as geometric means for three independent repeats with lower and upper geometric standard error of the Mean values in parentheses (see Ex-perimental for details).
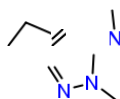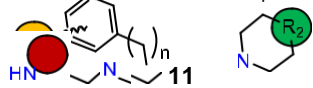


|      | R$^1$       | R$^2$                | n | IC$_{50}$ (μM)     | Calc. LogP[b] |
|------|-------------|----------------------|---|--------------------|---------------|
| **11a** | 2-MeO       | N-(CH$_2$)$_2$CH$_3$  | 0 | No activity[a]     | 3.96          |
| **11b** | 2-MeO       | N-(furan-2-carbonyl) | 1 | No activity[a]     | 2.62          |
| **11c** | 2-MeO       | N-CH$_2$CH$_3$        | 1 | ≫50                | 2.70          |
| **11d** | 2-MeO       | N-(CH$_2$)$_2$CH$_3$  | 1 | 7.35 (5.49, 9.83)  | 3.96          |
| **11e** | 4-MeO       | N-(CH$_2$)$_2$CH$_3$  | 1 | No activity[a]     | 3.25          |
| **11f** | 2,5-(MeO)$_2$ | N-(CH$_2$)$_2$CH$_3$ | 1 | No activity[a]     | 3.24          |
| **11g** | 3-Me        | N-(CH$_2$)$_2$CH$_3$  | 1 | No activity[a]     | 3.62          |
| **11h** | 2-Cl        | N-(CH$_2$)$_2$CH$_3$  | 1 | No activity[a]     | 3.83          |
| **11i** | 2-MeO       | N-(CH$_2$)$_2$OH      | 1 | No activity[a]     | 1.69          |
| **11j** | 2-MeO       | O                    | 1 | No activity[a]     | 2.28          |
| **11k** | 2-MeO       | CH-(piperidin-1-yl)  | 1 | 4.44 (3.66, 5.38)  | 3.76          |

[a] No activity means < 5% inhibition observed at highest concentration of compound [50 μM in 3.0% (v/v) DMSO].

[b] LogP values calculated using http://www.molinspiration.com/cgi-bin/properties.

pyrazolopyrimidines **11a-11k** (Table 2) were selected for further in-vestigation.

## 2.2. Characterization of inhibitor properties

Initially, the enzymatic activity was assayed with 50 μM **10a-10q** and **11a-11k** in the presence of 3.0% (v/v) DMSO. The upper con-centration in the pyrazoloquinoline series **10a-10q** was limited to 50 μM by solubility, as significant precipitation was observed at higher concentrations. Many compounds in the pyrazoloquinoline series **10a-10q** (Table 1) showed inhibition. On the other hand, most compounds in the pyrazolopyrimidine series **11a** – **11k** (Table 2) were inactive, with only two compounds (**11d** and **11k**) displaying significant in-hibitory activity.

Active compounds were subsequently analysed using dose-response curves, in the presence of 3.0% DMSO, in order to determine their IC$_{50}$ values (Tables 1 and 2). The most potent compounds (**10a**, **10i** and **10j**) had IC$_{50}$ values in the 1.5–2.3 μM range, which are similar values to those reported for some rationally designed inhibitors [28–32,37]. Analysis of the structure-activity relationships showed several inter-esting features. The phenyl ring bearing R$^1$ was generally not very tolerant of substitutions at the 3- or 4-positions. Introduction of a small substituent (F) at the 4-position resulted in a *ca.* 3-fold increase in the IC$_{50}$ (compound **10b** *vs.* **10a**), whilst introduction of a bulky OMe group (compound **10c** *vs.* **10a**) resulted in even more diminuation of in-hibitory activity. It is not clear if this phenomenon is a result of the steric or electron-withdrawing effect upon introduction of the fluorine. Fluorine has a relatively small van der Waals radius (*ca.* 1.35 Å), tra-ditionally viewed as similar to hydrogen (1.10 Å) [43,44]. Similarly, carbon-fluorine bonds (1.26–1.47 Å) are traditionally viewed as isos-teric with carbon-hydrogen bonds (1.08–1.2 Å) [43,45], but some stu-dies have suggested that carbon-fluorine bonds are more similar to carbon-oxygen bonds (1.52 Å) [44,45]. The high electronegativity of fluorine [43–45] and the increased lipophilicity of fluorine-containing compounds [43] have been extensively exploited in drug design. The compounds selected did not allow for direct evaluation of the effect of introducing a 3-F group but the results suggest that this substitution is also not particularly well tolerated (compounds **10d**, **10l** and **10n**). This

behaviour appears to primarily result from steric effects [43–45]. In contrast, substitutions at R$^2$ appear to be well tolerated. Matching of compounds suggests that R$^2$ = H, F or, Me or OMe has little effect on the observed IC$_{50}$. However, there are unexplained exceptions to this general rule, *e.g.* **10h** (R$^2$ = Me) has an IC$_{50}$ = 5.77 μM, whilst **10o** (which differs only in R$^2$ = F) is inactive (Table 1).

Substitution of the amide phenyl group (R$^3$) showed several inter-esting trends. Small groups, *e.g.* F, at the 4-position were well tolerated and appeared to increase potency (**10j** *vs.* **10b**). In contrast, addition of a larger group (OMe; **10e**), almost abolished inhibitory activity, al-though, in this case, the analysis is complicated by the simultaneous change of R$^2$ from F to Me. When R$^3$ = 3-F this resulted in a ~3-fold decrease in activity (compounds **10k**, **10l**, and **10n**). The presence of the larger group (OMe) had an inconsistent effect, as noted above, with **10h** having a similar activity to **10l**, whilst **10o** lost all activity. Finally, introduction of a 2-F group as R$^3$ almost abolished activity (compound **10m** *vs.* **10j**). Analysis of the side-chain amide moiety showed that substituting the phenyl ring with cyclohexyl- (compound **10p** *vs.* **10b**) decreased activity (IC$_{50}$ = 17.5 *vs.* 7.41 μM). Extending the side-chain with a methylene group (compound **10q** *vs.* **10b**; n = 1 *vs.* n = 0) re-sulted in almost complete loss of inhibitory activity (Table 1).

All of these compounds displayed reversible inhibition, as judged by rapid dilution experiments (Supporting Information). However, it was notable that most dose-response curves had Hill coefficients which were significantly higher than 1 with a few compounds having an average Hill coefficient of > 3 (**10b**, **10d**, **10g**, **10h** and **10i**) indicating that these compounds were not well-behaved inhibitors. We considered the possibility that inhibition of AMACR arose due to aggregation of com-pounds or other Pan-Assay Interference mechanisms [41,42]. Control experiments showed that inhibition was retained when assays were conducted in the presence of Triton X-100 (Supporting Information, Fig. S2), implying that compound aggregation was not a significant factor. Moreover, compounds were negative when analysed for Pan-Assay Interference properties [42]. We also considered whether the observed high H-coefficients arose due to problems with inhibitor so-lubility, and hence investigated whether $p$IC$_{50}$ values or Hill coefficients were correlated with LogP values but no trends were apparent (Supporting Information, Figs. S3 and S4). Kinetic analysis of inhibition by **10a** and **10j** (Supporting Information) was used to determine the type of inhibition. In the case of **10a** uncompetitive inhibition was observed, with a $K_i$ value of 4.8 ± 0.7 μM (mean ± S.E.M.) (*vide infra*). In contrast, mixed competitive inhibition was observed for **10j**, with a $K_i$ value of 2.4 ± 0.9 μM (mean ± S.E.M.), with α = 6.6. This latter behaviour is consistent with model in which the inhibitor binds to the adenosine site of the coenzyme A moiety.

In the case of the pyrazolopyrimidine series of compounds (**11a-11k**), only two examples (**11d** and **11k**) showed inhibition at 50 μM. It is striking that the inactive nine compounds had only minor structural differences compared to the active compounds (Table 2). Further ki-netic analysis of inhibition **11k** in the presence of 3.0% (v/v) DMSO showed that it was an uncompetitive inhibitor, with a $K_i$ value of 4.6 ± 0.4 μM (mean ± S.E.M.). This type of inhibition arises from exclusive binding of the inhibitor to the enzyme-substrate complex, with no significant binding to enzyme alone [46]. This behaviour is inconsistent with a mode of action in which the inhibitor binds to the site occupied by the adenosine moiety of the CoA because the inhibitor binds only to the enzyme-substrate complex. The crystal structures of MCR [11–13] show that the enzyme is a dimer, with basic side-chains in the active site catalysing deprotonation and reprotonation contributed by both subunits. Theoretically, uncompetitive inhibition could occur by **10a** or **11k** binding to one active site whilst the other is occupied by substrate. However, this requires that substrate binding to subunits is cooperative and there is no evidence that this is the case (Hill coeffi-cient is ~1 when kinetic data is fitted to the cooperative model). The mode of action is therefore unclear at this time but it could be that the inhibitor binds between the two dimer subunits and this may explain

why many analogues of **11k** are inactive (Table 2).

## 3. Conclusions

The new colorimetric assay [28,37] allows rapid identification of inhibitors by high-throughput screening. The assay is simple to use, consisting of mixing of the enzyme and drug stock solutions followed by addition of substrate stock solution after the desired pre-incubation period. Monitoring formation of product over time allows convenient characterization of inhibitory properties, including $IC_{50}$ and $K_i$ values, and determining whether the inhibitor is reversible or not. For optimum sensitivity, a kinetic assay is used, although the assay is sufficiently sensitive to use an end-point format. A disadvantage of the end-point format is that many potential inhibitors absorb at 354 nm and this complicates analysis of the results. Our reported assay contrasts with the radiochemical assay used for high-throughput screening of AMACR reported by Wilson *et al.* in 2011 [22], which required multiple steps and physical separation of the products using column chromatography. Our study also differs in that the discovered inhibitors are not non-specific protein-modifying agents, in contrast to the compounds re-ported by Wilson *et al.* [22].

This study identifies pyrazoloquinolines and pyrazolopyrimidines as new classes of AMACR inhibitor. The libraries of drug-like compounds used in this screening study were provided by LifeArc [40]. Similar compounds to those identified in this study have been reported as in-hibitors of various kinases [47–53] and also of bacterial cell-wall bio-synthetic enzymes which use UDP derivatives as substrates [54]. However, this appears to be the first report of such compounds in-hibiting an enzyme using an acyl-CoA substrate. Kinetic analysis of pyrazoloquinoline inhibitor **10j** showed that it was mixed competitive, consistent with it binding to the same site as the adenosine moiety of the CoA as well as to the enzyme substrate complex. In contrast, the pyrazoloquinoline inhibitor **10a** and the pyrazolopyrimidine inhibitor **11k** were uncompetitive. These appear to be the first examples of un-competitive AMACR inhibitors, while all other characterized reversible inhibitors been competitive [28]. Uncompetitive inhibition offers sig-nificant advantages over other types of inhibition for pharmacological applications in that inhibition is increased at high substrate con-centrations compared to low substrate concentrations [46]. This means that inhibition of the enzyme within the cell is not eventually overcome by the build-up of substrate and precursors. The results of this paper demonstrate that our high-throughput screening assay is suitable for identifying novel, 'druggable' compounds as AMACR inhibitors.

## 4. Materials and methods

### 4.1. Sources of materials

Chemicals were purchased from the Sigma-Aldrich Chemical Co. or Fisher Scientific Ltd., unless otherwise stated, and were used without further purification. Reduced coenzyme A, tri-lithium salt, was pur-chased from Calbiochem. High-throughput screening libraries were obtained as 1.0 mM solutions in DMSO from LifeArc in 384-well plates [40]. Human recombinant AMACR 1A was expressed and purified and substrate **7** was synthesized as previously described [28]. Inhibitors **10** and **11** were obtained from Chemdiv; ^{1}H NMR and mass spectrometric data for these compounds (Supporting Information) were supplied by Chemdiv.

### 4.2. High-throughput screening

A protocol modified from that previously reported assay based on elimination of 2,4-dinitrophenolate **8** [28,37] was used to screen the libraries. A multi-channel pipette was used to add 6.0 µL of stock so-lution of inhibitor in DMSO into a 96 well plate, followed by 294 µL of enzyme stock solution in 50 mM aq. $NaH_2PO_4$-NaOH, pH 7.4. Following

10 min incubation at ambient temperature, the mixture was divided into 3 × 100 µL and the enzymatic reaction was initiated by adding 2 × substrate stock solution (3 × 100 µL) in the same buffer with the plate incubated at 30 °C. Final concentrations in the assay of potential inhibitor, DMSO, substrate **7** and enzyme were 30 µM, 3.0% (v/v), 40 µM, and ~0.04 $mg.mL^{-1}$, respectively. Formation of product was followed at 354 nm (and 390 nm) for 8 min, using a BMG Labtech FLUOstar Omega plate reader with Omega software. Potential hits were rescreened under the same conditions and compared to positive (en-zyme + DMSO) and negative controls (buffer + DMSO). Under these conditions, Z′ = 0.71 ± 0.13 (mean ± standard deviation, three in-dependent repeats) for measurement at 354 nm. Some assays were conducted in 96 well half-volume plates, in a final volume of 100 µL with the same reagent concentrations. Control assays show identical results with both types of plate [28].

### 4.3. Evaluation of AMACR inhibition

Colorimetric assays were performed as previously described [28,37]. Assays were typically conducted in half-volume 96-well plates, in a final volume of 100 µL. Each assay mixed 9.0 µL DMSO stock and 141 µL enzyme stock. After 10 min, this was divided into 3 × 50 µL and the assay was initiated by addition of 3 × 50 µL of colorimetric sub-strate **7** in buffer. The following final concentrations were used in dose-response curves: inhibitors, 50, 16.7, 5.55, 1.85, 0.617, 0.205, 0.068 and 0.022 µM; DMSO, 3% (v/v); substrate, 40 µM; and enzyme, 0.0396 $mg\ mL^{-1}$. Reaction rates were determined by plotting $A_{354}$ with time in Excel [28] and data were analysed using SigmaPlot 13. $Log_{10}$ $IC_{50}$ values were calculated from individual dose-response curves with inhibition of binding plotted against $Log_{10}$ drug concentration (in M). Mean $Log_{10}$ $IC_{50}$ values were then calculated from 3 repeats together with corresponding $Log_{10}$ Standard Error of the Mean (S.E.M.) values. Data were then converted to non-logarithmic values to produce the geometric mean with corresponding upper and lower limits of the geometric S.E.M. values (in µM); see Tables 1 and 2. Compounds were screened for Pan-Activity Inhibition using the following websites: https://www.cbligand.org/PAINS/ [42] and http://zinc15.docking.org/patterns/home/.

Reversibility experiments (See Supporting Information) used in-hibitor at *ca.* 10 × $IC_{50}$ value in experiment 1, with all other reagents at the above concentrations and a 100 µL final volume. Experiment 2 used concentrated enzyme (1.69 $mg\ mL^{-1}$) which was incubated with in-hibitor and DMSO at the same concentrations as in Experiment 1. After 10 min, the mixture was diluted with 6.0% (v/v) DMSO to give the same enzyme concentration as in Experiment 1 and 3 × 50 µL was placed in the plate. Substrate stock solution (3 × 50 µL) was added to the diluted enzyme/drug mixture and the reaction was followed at 354 nm for 15.5 min. Average $A_{354}$ values and standard deviations (n = 3) were calculated in Excel [28]. Positive controls contained en-zyme + DMSO and negative controls contained buffer + DMSO.

The $K_i$ value for **10a** was determined at a fixed concentration of 0, 1.43, 2.31 and 3.71 µM in the assay. For **10j** a fixed concentration of 0, 0.87, 1.52 and 2.65 µM were used. Rates were determined at 354 nm for eight concentrations of substrate (100, 66.6, 44.4, 29.6, 19.7, 13.2, 8.7 and 5.85 µM final concentration in assay); in the case of **10a** and **10j** significant substrate inhibition was observed at higher substrate con-centrations. Therefore, the 5 or 6 of the lowest substrate concentrations were used in this analysis. DMSO and enzyme concentrations were 3.0% (v/v), and 0.0396 $mg\ mL^{-1}$, respectively. The $K_i$ value for **11k** was determined using a fixed concentration of 0, 1.24, 4.44 and 15.88 µM. The same substrate, DMSO and enzyme concentration was used as above. Rates were determined in Excel, as above, and kinetic parameters determined using SigmaPlot 13 with the exploratory EK and enzyme kinetics modules. Inhibitory mode was decided by visual in-spection of plots and ranking of solutions by SigmaPlot 13.

## Funding

## Declaration of Competing Interest

MY, MDT, TJW and MDL are named inventors on patent applications on the use and application of the colorimetric assay. The other authors report no competing interests.

## Note

The authors are members of the Cancer Research @ Bath (CR@B) network.

## Acknowledgements

## Appendix A. Supplementary material

Supplementary data to this article can be found online at https://doi.org/10.1016/j.bioorg.2019.103264.

## References

[1] M.D. Lloyd, D.J. Darley, A.S. Wierzbicki, M.D. Threadgill, α-Methylacyl-CoA race-mase: an 'obscure' metabolic enzyme takes centre stage, FEBS J. 275 (2008) 1089–1102.

[2] M.D. Lloyd, M. Yevglevskis, G.L. Lee, P.J. Wood, M.D. Threadgill, T.J. Woodman, α-Methylacyl-CoA racemase (AMACR): metabolic enzyme, drug metabolizer and cancer marker P504S, Prog. Lipid Res. 52 (2013) 220–230.

[3] M. Mukherji, C.J. Schofield, A.S. Wierzbicki, G.A. Jansen, R.J.A. Wanders, M.D. Lloyd, The chemical biology of branched-chain lipid metabolism, Prog. Lipid Res. 42 (2003) 359–376.

[4] R.J.A. Wanders, Metabolic functions of peroxisomes in health and disease, Biochimie 98C (2014) 36–44.

[5] K.P. Battaile, M. McBurney, P.P. Van Veldhoven, J. Vockley, Human long chain, very long chain and medium chain acyl-CoA dehydrogenases are specific for the S-enantiomer of 2-methylpentadecanoyl-CoA, Biochim. Biophys. Acta -Lipids Lipid Metabol. 1390 (1998) 333–338.

[6] P.P. VanVeldhoven, K. Croes, S. Asselberghs, P. Herdewijn, G.P. Mannaerts, Peroxisomal β-oxidation of 2-methyl-branched acyl-CoA esters: Stereospecific re-cognition of the 2S-methyl compounds by trihydroxycoprostanoyl-CoA oxidase and pristanoyl-CoA oxidase, FEBS Lett. 388 (1996) 80–84.

[7] P.P. Van Veldhoven, K. Croes, M. Casteels, G.P. Mannaerts, 2-Methylacyl racemase: a coupled assay based on the use of pristanoyl-CoA oxidase/peroxidase and re-investigation of its subcellular distribution in rat and human liver, Biochim. Biophys. Acta-Lipids Lipid Metab. 1347 (1997) 62–68.

[8] N. Hoshita, S. Shefer, F.W. Cheng, B. Dayal, A.K. Batta, G.S. Tint, G. Salen, E.H. Mosbach, Biosynthesis of chenodeoxycholic acid - Side-chain hydroxylation of 5-β-cholestane-3-α-,7-α-diol by subcellular fractions of guinea pig liver, Lipids 13 (1978) 961–965.

[9] D.J. Darley, D.S. Butler, S.J. Prideaux, T.W. Thornton, A.D. Wilson, T.J. Woodman, M.D. Threadgill, M.D. Lloyd, Synthesis and use of isotope-labelled substrates for a mechanistic study on human α-methylacyl CoA racemase 1A (AMACR; P504S), Org. Biomol. Chem. 7 (2009) 543–552.

[10] T.J. Woodman, P.J. Wood, A.S. Thompson, T.J. Hutchings, G.R. Steel, P. Jiao, M.D. Threadgill, M.D. Lloyd, Chiral inversion of 2-arylpropionyl-CoA esters by α-methylacyl-CoA racemase 1A (AMACR; P504S), Chem. Commun. 47 (2011) 7332–7334.

[11] P. Bhaumik, W. Schmitz, A. Hassinen, J.K. Hiltunen, E. Conzelmann, R.K. Wierenga, The catalysis of the 1,1-proton transfer by α-methyl-acyl-CoA racemase is coupled to a movement of the fatty acyl moiety over a hydrophobic, methionine-rich sur-face, J. Mol. Biol. 367 (2007) 1145–1161.

[12] K. Savolainen, P. Bhaumik, W. Schmitz, T.J. Kotti, E. Conzelmann, R.K. Wierenga, J.K. Hiltunen, α-Methylacyl-CoA racemase from Mycobacterium tuberculosis: muta-tional and structural characterization of the active site and the fold, J. Biol. Chem. 280 (2005) 12611–12620.

[13] S. Sharma, P. Bhaumik, W. Schmitz, R. Venkatesan, J.K. Hiltunen, E. Conzelmann, A.H. Juffer, R.K. Wierenga, The enolization chemistry of a thioester-dependent racemase: the 1.4 Å crystal structure of a reaction intermediate complex characterized by detailed QM/MM calculations, J. Phys. Chem. B 116 (2012) 3619–3629.

[14] X. Li, Q.-C. Zheng, H.-X. Zhang, Quantum chemical modeling of 1,1-proton transfer reaction catalyzed by a cofactor-independent α-methylacyl-CoA racemase, Int. J. Quantum Chem. 112 (2012) 619–624.

[15] J. Luo, S. Zha, W.R. Gage, T.A. Dunn, J.L. Hicks, C.J. Bennett, C.N. Ewing, E.A. Platz, S. Ferdinandusse, R.J. Wanders, J.M. Trent, W.B. Isaacs, A.M. De Marzo, α-Methylacyl-CoA racemase: a new molecular marker for prostate cancer, Cancer Res. 62 (2002) 2220–2226.

[16] C. Kumar-Sinha, R.B. Shah, B. Laxman, S.A. Tomlins, J. Harwood, W. Schmitz, E. Conzelmann, M.G. Sanda, J.T. Wei, M.A. Rubin, A.M. Chinnaiyan, Elevated α-methylacyl-CoA racemase enzymatic activity in prostate cancer, Am. J. Pathol. 164 (2004) 787–793.

[17] A.K. Witkiewicz, S. Varambally, R. Shen, R. Mehra, M.S. Sabel, D. Ghosh, A.M. Chinnaiyan, M.A. Rubin, C.G. Kleer, α-Methylacyl-CoA racemase protein ex-pression is associated with the degree of differentiation in breast cancer using quantitative image analysis, Cancer Epidemiol. Biomarkers Prev. 14 (2005) 1418–1423.

[18] C.-F. Li, F.-M. Fang, J. Lan, J.-W. Wang, H.-J. Kung, L.-T. Chen, T.-J. Chen, S.-H. Li, Y.-H. Wang, H.-C. Tai, S.-C. Yu, H.-Y. Huang, AMACR amplification in myxofi-brosarcomas: a mechanism of overexpression that promotes cell proliferation with therapeutic relevance, Clin. Cancer Res. 20 (2014) 6141–6152.

[19] Z. Jiang, G.R. Fanger, B.F. Banner, B.A. Woda, P. Algate, K. Dresser, J.C. Xu, S.G. Reed, K.L. Rock, P.G. Chu, A dietary enzyme: α-methylacyl-CoA racemase/ P504S is overexpressed in colon carcinoma, Cancer Detect. Prev. 27 (2003) 422–426.

[20] Z. Jiang, G.R. Fanger, B.A. Woda, B.F. Banner, P. Algate, K. Dresser, J.C. Xu, P.G. Chu, Expression of α-methylacyl-CoA racemase (P504S) in various malignant neoplasms and normal tissues: a study of 761 cases, Human Pathol. 34 (2003) 792–796.

[21] S. Zha, S. Ferdinandusse, S. Denis, R.J. Wanders, C.M. Ewing, J. Luo, A.M. De Marzo, W.B. Isaacs, α-Methylacyl-CoA racemase as an androgen-independent growth modifier in prostate cancer, Cancer Res. 63 (2003) 7365–7376.

[22] B.A.P. Wilson, H. Wang, B.A. Nacev, R.C. Mease, J.O. Liu, M.G. Pomper, W.B. Isaacs, High-throughput screen identifies novel inhibitors of cancer biomarker α-methylacyl-coenzyme A racemase (AMACR/P504S), Mol. Cancer Ther. 10 (2011) 825–838.

[23] K. Takahara, H. Azuma, T. Sakamoto, S. Kiyama, T. Inamoto, N. Ibuki, T. Nishida, H. Nomi, T. Ubai, N. Segawa, Y. Katsuoka, Conversion of prostate cancer from hormone independency to dependency due to AMACR inhibition: involvement of increased AR expression and decreased IGF1 expression, Anticancer Res. 29 (2009) 2497–2505.

[24] S.E. Daugherty, Y.Y. Shugart, E.A. Platz, M.D. Fallin, W.B. Isaacs, R.M. Pfeiffer, R. Welch, W.-Y. Huang, D. Reding, R.B. Hayes, Polymorphic variants in α-methy-lacyl-CoA racemase and prostate cancer, Prostate 67 (2007) 1487–1497.

[25] S.E. Daugherty, E.A. Platz, Y.Y. Shugart, M.D. Fallin, W.B. Isaacs, N. Chatterjee, R. Welch, W.Y. Huang, R.B. Hayes, Variants in the α-methylacyl-CoA racemase gene and the association with advanced distal colorectal adenoma, Cancer Epidemiol. Biomarkers Prev. 16 (2007) 1536–1542.

[26] K.S. Lee, S.M. Park, K.H. Rhee, W.G. Bang, K. Hwang, Y.M. Chi, Crystal structure of fatty acid-CoA racemase from Mycobacterium tuberculosis H37Rv, Prot. Struct. Funct. Bioinform. 64 (2006) 817–822.

[27] M. Yevglevskis, G.L. Lee, J. Sun, S. Zhou, X. Sun, G. Kociok-Köhn, T.D. James, T.J. Woodman, M.D. Lloyd, A study on the AMACR catalysed elimination reaction and its application to inhibitor testing, Org. Biomol. Chem. 14 (2016) 612–622.

[28] M. Yevglevskis, G.L. Lee, A. Nathubhai, Y.D. Petrova, T.D. James, M.D. Threadgill, T.J. Woodman, M.D. Lloyd, A novel colorimetric assay for α-methylacyl-CoA ra-cemase 1A (AMACR; P504S) utilizing the elimination of 2,4-dinitrophenolate, Chem. Commun. 53 (2017) 5087–5090.

[29] A.J. Carnell, I. Hale, S. Denis, R.J.A. Wanders, W.B. Isaacs, B.A. Wilson, S. Ferdinandusse, Design, synthesis, and in vitro testing of α-methylacyl-CoA race-mase inhibitors, J. Med. Chem. 50 (2007) 2700–2707.

[30] A.J. Carnell, R. Kirk, M. Smith, S. McKenna, L.-Y. Lian, R. Gibson, Inhibition of human α-methylacyl-CoA racemase (AMACR): a target for prostate cancer, ChemMedChem 8 (2013) 1643–1647.

[31] A. Morgenroth, E.A. Urusova, C. Dinger, E. Al-Momani, T. Kull, G. Glatting, H. Frauendorf, O. Jahn, F.M. Mottaghy, S.N. Reske, B.D. Zlatopolskiy, New mole-cular markers for prostate tumor imaging: a study on 2-methylene substituted fatty acids as new AMACR inhibitors, Chem. Eur. J. 17 (2011) 10144–10150.

[32] C. Festuccia, G.L. Gravina, A. Mancini, P. Muzi, E. Di Cesare, R. Kirk, M. Smith, S. Hughes, R. Gibson, L.-Y. Lian, E. Ricevuto, A.J. Carnell, Trifluoroibuprofen in-hibits alpha-methylacyl coenzyme A racemase (AMACR/P504S), reduces cancer cell proliferation and inhibits in vivo tumor growth in aggressive prostate cancer models, Anti-Cancer Ag. Med. Chem. 14 (2014) 1031–1041.

[33] M. Pal, N.M. Easton, H. Yaphe, S.L. Bearne, Potent dialkyl substrate-product ana-logue inhibitors and inactivators of α-methylacyl-coenzyme A racemase from Mycobacterium tuberculosis by rational design, Bioorg. Chem. 77 (2018) 640–650.

[34] M. Pal, M. Khanal, R. Marko, S. Thirumalairajan, S.L. Bearne, Rational design and synthesis of substrate-product analogue inhibitors of α-methylacyl-coenzyme A racemase from Mycobacterium tuberculosis, Chem. Commun. 52 (2016) 2740–2743.

[35] C.A. Lipinski, F. Lombardo, B.W. Dominy, P.J. Feeney, Experimental and compu-tational approaches to estimate solubility and permeability in drug discovery and development settings, Adv. Drug Deliv. Rev. 23 (1997) 3–25.

[36] C.A. Lipinski, F. Lombardo, B.W. Dominy, P.J. Feeney, Experimental and compu-tational approaches to estimate solubility and permeability in drug discovery and development settings, Adv. Drug Deliv. Rev. 46 (2001) 3–26.

[37] M. Yevglevskis, G.L. Lee, A. Nathubhai, Y.D. Petrova, T.D. James, M.D. Threadgill, T.J. Woodman, M.D. Lloyd, Structure-activity relationships of rationally designed AMACR 1A inhibitors, Bioorg. Chem. 79 (2018) 145–154.

[38] R.A. Copeland, Mechanistic considerations in high-throughput screening, Anal. Biochem. 320 (2003) 1–12.

[39] J.H. Zhang, T.D.Y. Chung, K.R. Oldenburg, A simple statistical parameter for use in evaluation and validation of high throughput screening assays, J. Biomol. Screening 4 (1999) 67–73.

[40] K. Birchall, A. Merritt, A. Sattikar, C. Kettleborough, B. Saxty, Design of the LifeArc index set and retrospective review of its performance: a collection for sharing, SLAS Discov. 24 (2019) 332–345.

[41] C. Aldrich, C. Bertozzi, G.I. Georg, L. Kiessling, C. Lindsley, D. Liotta, K.M. Merz, A. Schepartz, S.M. Wang, The ecstasy and agony of assay interference compounds, J. Med. Chem. 60 (2017) 2165–2168.

[42] J.B. Baell, G.A. Holloway, New substructure filters for removal of pan assay interference compounds (PAINS) from screening libraries and for their exclusion in bioassays, J. Med. Chem. 53 (2010) 2719–2740.

[43] J. Mann, Modern methods for the introduction of fluorine into organic molecules: an approach to compounds with altered chemical and biological activities, Chem. Soc. Rev. 16 (1987) 381–436.

[44] R. Pongdee, H.W. Liu, Elucidation of enzyme mechanisms using fluorinated sub-strate analogues, Bioorg. Chem. 32 (2004) 393–437.

[45] K.L. Kirk, Fluorine in medicinal chemistry: recent therapeutic applications of fluorinated small molecules, J. Fluorine Chem. 127 (2006) 1013–1029.

[46] R.A. Copeland, Evaluation of enzyme inhibitors in drug discovery. A guide for medicinal chemists and pharmacologists, John Wiley & Sons, Inc., Hoboken, New Jersey, 2005.

[47] M.T. El Sayed, H.A.R. Hussein, N.M. Elebiary, G.S. Hassan, S.M. Elmessery, A.R. Elsheakh, M. Nayel, H.A. Abdel-Aziz, Tyrosine kinase inhibition effects of novel pyrazolo[1,5-a]pyrimidines and pyrido[2,3-d]pyrimidines ligand: synthesis, biological screening and molecular modeling studies, Bioorg. Chem. 78 (2018) 312–323.

[48] S.J. Ma, S.F. Zhou, W.C. Lin, R. Zhang, W.J. Wu, K.C. Zheng, Study of novel pyrazolo[3,4-d] pyrimidine derivatives as selective TgCDPK1 inhibitors: molecular docking, structure-based 3D-QSAR and molecular dynamics simulation, RSC Adv. 6 (2016) 100772–100782.

[49] B. Pujala, A.K. Agarwal, S. Middya, M. Banerjee, A. Surya, A.K. Nayak, A. Gupta, S. Khare, R. Guguloth, N.A. Randive, B.U. Shinde, A. Thakur, D.I. Patel, M. Raja, M.J. Green, J. Alfaro, P. Avila, F. Pérez de Arce, R.G. Almirez, S. Kanno, S. Bernales, D.T. Hung, S. Chakravarty, E. McCullagh, K.P. Quinn, R. Rai, S.M. Pham, Discovery of pyrazolopyrimidine derivatives as novel dual inhibitors of BTK and PI3K δ, ACS Med. Chem. Lett. 7 (2016) 1161–1166.

[50] F.U. Rutaganira, J. Barks, M. Savari Dhason, Q. Wang, M.S. Lopez, S. Long, J.B. Radke, N.G. Jones, A.R. Maddirala, J.W. Janetka, M. El Bakkouri, R. Hui, K.M. Shokat, L.D. Sibley, Inhibition of calcium dependent protein kinase 1 (CDPK1) by pyrazolopyrimidine analogs decreases establishment and reoccurrence of central nervous system disease by Toxoplasma gondii, J. Med. Chem. 60 (2017) 9976–9989.

[51] R. Tripathy, R.J. McHugh, A.K. Ghose, G.R. Ott, T.S. Angeles, M.S. Albom, Z. Huang, L.D. Aimone, M. Cheng, B.D. Dorsey, Pyrazolone-based anaplastic lym-phoma kinase (ALK) inhibitors: control of selectivity by a benzyloxy group, Bioorg. Med. Chem. Lett. 21 (2011) 7261–7264.

[52] R.P. Wurz, L.H. Pettus, B. Henkle, L. Sherman, M. Plant, K. Miner, H.J. McBride, L.M. Wong, C.J.M. Saris, M.R. Lee, S. Chmait, C. Mohr, F. Hsieh, A.S. Tasker, Part 2: Structure-activity relationship (SAR) investigations of fused pyrazoles as potent, selective and orally available inhibitors of p38α mitogen-activated protein kinase, Bioorg. Med. Chem. Lett. 20 (2010) 1680–1684.

[53] R.P. Wurz, L.H. Pettus, S.M. Xu, B. Henkle, L. Sherman, M. Plant, K. Miner, H. McBride, L.M. Wong, C.J.M. Saris, M.R. Lee, S. Chmait, C. Mohr, F. Hsieh, A.S. Tasker, Part 1: Structure-Activity Relationship (SAR) investigations of fused pyrazoles as potent, selective and orally available inhibitors of p38α mitogen-activated protein kinase, Bioorg. Med. Chem. Lett. 19 (2009) 4724–4728.

[54] V. Humnabadkar, K.R. Prabhakar, A. Narayan, S. Sharma, S. Guptha, P. Manjrekar, M. Chinnapattu, V. Ramachandran, S.P. Hameed, S. Ravishankar, M. Chatterji, UDP-N-Acetylmuramic acid L-alanine ligase (MurC) inhibition in a tolC mutant Escherichia coli strain leads to cell death, Antimicrob. Agents Chemother. 58 (2014) 6165–6171.